Introduction

1.1 From ancient astronomy to modern astrochemistry

Mankind has ever been fascinated with the stars. Dating back to the most ancient of times, human life has been governed by the endless cycles of day and night and of winter, spring, summer and fall. Already in the early Stone Age, people must have seen a relationship between the rising and setting of the Sun on the one hand, and dark turning into light turning back into dark on the other hand. Having established the Sun as the cause of light and warmth, it is a logical next step to wonder whether other objects in the sky could equally influence life on Earth. As George Forbes wrote in his book *History of Astronomy* (1909), "this led to a search for other signs in the heavens. If the appearance of a comet was sometimes noted simultaneously with the death of a great ruler, or an eclipse with a scourge of plague, these might well be looked upon as causes in the same sense that the veering or backing of the wind is regarded as a cause of fine or foul weather."

With today's knowledge, it is easy to say that comets, eclipses and most other astronomical phenomena do not altogether affect our lives as much as our ancestors believed. Nonetheless, their suppositions led them to keep detailed records of anything remarkable taking place in the sky. Clay tablets surviving from Babylonia show that people were keeping track of solar eclipses at least as far back as 1062 B.C. (Cowell 1905). In China, c. 2450 B.C., the emperor Zhuanxu apparently saw a conjunction of Mercury, Mars, Saturn and Jupiter on the same day that the Moon was in conjunction with the Sun (Chambers 1889, Hail & Leavens 1940). The preferential east-west and north-south alignment of graves and bodies in burial sites from the late Stone Age suggests that mankind was engaged in primitive astronomy as early as 4500 B.C. (Schmidt-Kaler & Schlosser 1984).

If the Babylonians laid the foundations for modern astronomy, it was the Greek who started building in earnest. From around 600 B.C. onwards, scholars like Thales, Pythagoras, Anaxagoras, Plato and Eratosthenes performed many revolutionary measurements and observations, and devised many equally revolutionary theories about the Earth and the Moon, the planets, and the Sun and the stars (Lewis 1862). The most prolific of the Greek astronomers was Hipparchus (c. 190–120 B.C.), regarded by Forbes (1909) as the founder of observational astronomy. Amongst other contributions, he compiled the first comprehensive star catalogue and discovered the precession of the Earth's axis. Another key figure from the classical period is the Roman Ptolemy, who, around 150 A.D., wrote one of the first textbooks on astronomy. Known as the *Almagest* or the *Great Treatise*, it contained a summary of the astronomical knowledge then available, including a detailed model of the motions of the Sun, the planets and the stars.

Hipparchus, Ptolemy and all astronomers before them were mostly concerned with the motions of the stars and the planets, and not so much with their physical nature. After all, astronomy as a science was born out of a desire to be able to predict signs in the skies that might announce a good harvest or the start of a war. In 1608, almost a millennium and a half after Ptolemy's *Almagest*, the three Dutchmen Hans Lippershey, Zacharias Janssen and Jacob Metius invented the telescope (van Helden 2009). This allowed Galileo Galilei (1564–1642) to embark on a whole new kind of astronomy. Suddenly, the Sun was known to have dark spots on its surface, Venus to have phases, Jupiter to have moons, and the Milky Way to consist of countless individual stars (Drake 1978).

Galileo's observations supported the heliocentric theory published by Nicolaus Copernicus in his 1543 work *De Revolutionibus Orbium Coelestium*, and scientists were now gradually accepting the idea of a spherical Earth orbiting the Sun in a vast expanse. This inevitably led to questions about the nature of the space between the planets and the stars. Sir Francis Bacon appears to have been the first to publish on this topic. In his *Descriptio Globi Intellectualis* (1653), he wrote, "Another question is, *what is contained in the interstellar spaces?* For they are either empty, as Gilbert thought; or filled with a body which is to the stars what air is to flame (...); or filled with a body homogeneous with the stars themselves, lucid and almost empyreal, but in a less degree (...)."[1] Despite Bacon's excellent ideas – his third option is remarkably close to the truth – it was not until the early 20th century that astronomers widely started to think of interstellar space as a very dilute gas. The first strong evidence of interstellar material came with the discovery of a very narrow calcium absorption line towards δ Orionis, which Hartmann (1904) concluded had to be due to a cloud of calcium gas located somewhere between Earth and this star. Independent of him, Kapteyn (1909) theorised that "interstellar space must contain, at every moment, a considerable amount of gas," based on the coronal gas expelled by the Sun and, presumably, other stars. The "dark markings of the sky" observed by Barnard (1919) provided further evidence of interstellar material, as did spectroscopic observations by Heger (1919), Beals (1936) and Dunham (1937a,b) and theoretical considerations by Birkeland (1913) and Thorndike (1930).

Now that astronomers knew there was an interstellar medium (ISM), they set out to identify its chemical composition. The observations so far had established the presence of Na, K, Ca^+, Ti^+ and other metal atoms and ions.[2] It was soon suggested the ISM might also contain simple molecules (Eddington 1926, Russell 1935, Swings 1937, Saha 1937), and this hypothesis was confirmed by the detections of CH (Swings & Rosenfeld 1937), CN (McKellar 1940) and CH^+ (Douglas & Herzberg 1941). Astrochemistry had arrived.

The advent of radio and microwave astronomy in the 1960s, followed by infrared astronomy in the late 1970s, provided a great boost for this fledgling area of science. By the time Neil Armstrong set foot on the Moon, the detection of OH, NH_3, H_2O and H_2CO had increased the number of confirmed interstellar molecules to seven (Weinreb 1963, Cheung et al. 1968, 1969, Snyder et al. 1969). Seven more were known within a year and a half, including two of the most abundant ones: H_2 and CO (Carruthers 1970, Wilson et al. 1970). The 50th and 100th space molecules were detected in 1978 (NO, by Liszt & Turner) and 1992 (SO^+, by Turner). Meanwhile, strong evidence had arisen for the ubiquitous presence of a class of much larger molecules known as polycyclic aromatic hydrocarbons or PAHs (Fig. 1.1; Gillett et al. 1973, Puget & Leger 1989, Allamandola et al. 1989, Tielens 2008), although as of yet no individual members of this class have been

---

[1] The quote comes from Bacon's collected and translated works, edited by Spedding, Ellis and Heath. The possibility of space being empty refers to William Gilbert's hypothesis in his *De Magnete* (1600; translated by Mottelay) that "the space above the earth's exhalations is a vacuum."

[2] Worth mentioning here is nebulium or nebulum, an element conjured up by Sir William Huggins in the 1860s to designate, as Clerke (1898) put it, "the exotic *world-stuff* originating the chief nebular ray at λ 5007 [and] its companion at λ 4959." Nebulium continued to be considered a common component of the ISM until Bowen (1928) showed that the lines at 5007 and 4959 Å were in fact due to doubly ionised oxygen, prompting Russell (1932) to quip that "nebulium [had] thus very literally vanished into thin air".
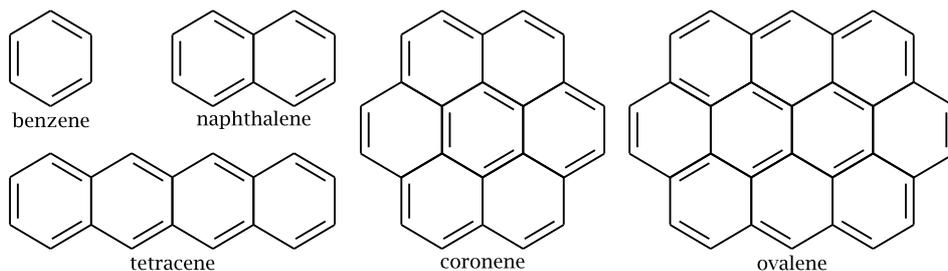
Figure 1.1 – A selection of polycyclic aromatic hydrocarbons (PAHs): benzene (C_6H_6), naphthalene ($C_{10}H_8$), tetracene ($C_{18}H_{12}$), coronene ($C_{24}H_{12}$) and ovalene ($C_{32}H_{14}$). Each corner represents a carbon atom; hydrogen atoms are not drawn.

firmly identified. The counter of interstellar and circumstellar molecules and molecular ions currently stands at 162 (Woon 2009), and astrochemistry has firmly established itself as an important field of research.[3]

1.2   Low-mass star formation and the role of chemistry

The ISM is now understood to consist of several components (Field et al. 1969, McKee & Ostriker 1977, Ferrière 2001). By volume, the top three are the hot ionised medium (particle density of 10^{-4}–10^{-2} cm^{-3}, temperature of 10^6–10^7 K), the warm ionised medium (0.2–0.5 cm^{-3}, 8000 K) and the warm neutral medium (0.2–0.5 cm^{-3}, 6000–10 000 K), together accounting for 95–99%. Most of the remaining volume is taken up by the cold neutral medium (20–50 cm^{-3}, 50–100 K). The densest ISM component, with a fractional volume of less than 1%, are the molecular clouds (10^2–10^6 cm^{-3}, 10–20 K). They are of particular importance for this thesis, as they are the birthplace of new stars.

Molecular clouds range in diameter from a few to maybe 10 or 20 pc and have a mass between 10^3 and 10^4 $M_\odot$ (Cambrésy 1999). They tend to be irregularly shaped and their density distribution is far from homogeneous. Embedded in molecular clouds are so-called clumps with typical densities of 10^3–10^4 cm^{-3} and typical diameters of 0.3–3 pc (Loren 1989, Williams et al. 1994). The clumps in turn harbour the so-called cores, whose densities are another order of magnitude higher and whose diameters are another order of magnitude smaller (Motte et al. 1998, Jijina et al. 1999, Caselli et al. 2002). The temperature in all these substructures is about 10 K (Bergin & Tafalla 2007).

Supported by pressure, turbulence and magnetic fields, cloud cores usually survive for a few 10^5 to possibly several 10^6 yr. They consist of a mixture of gas and tiny dust grains (radius of about 0.1 μm) in a mass ratio of 1 to 0.01, or a number ratio of 1 to 10^{-12} (Spitzer

---

[3] The list of 162 molecules includes various isomers, but no isotopologues. It contains no PAHs except the tentatively detected benzene (C_6H_6). It also contains other tentative and disputed detections such as glycine (NH_2CH_2COOH) and 1,3-dihydroxyacetone ($CO(CH_2OH)_2$).

1954, Kimura et al. 2003).[4] An active chemistry is already taking place during this stage. First of all, the initially atomic gas – inherited from the more diffuse ISM out of which the cloud coalesced – is transformed into simple molecules like CO, OH and N_2. Because of the low temperature and moderately high density, most of these molecules freeze out onto the dust. The resulting ice mantles offer the possibility for additional chemical reactions, leading for example to CO_2, CH_4, H_2O, H_2CO and CH_3OH (Watanabe & Kouchi 2002, Ioppolo et al. 2008, 2009, Fuchs et al. 2009).

The various physical and chemical stages involved in the formation of low-mass stars are illustrated in Fig. 1.2. Point 0 represents the cold phase of the static cloud core. As described in more detail in the rest of this section, the formation of a star at the centre of the core is initially accompanied by a warm-up of the surrounding material. At a later stage, when a dense disk is formed around the star, the temperature decreases again in some areas. The range of physical conditions encountered throughout the star-formation process results in a complex chemical evolution of both the gas and the dust.

The collapse of the core under its own gravity is initiated by the loss of turbulent or magnetic support. Material starts falling in towards the centre along trajectories such as the one drawn in Fig. 1.2. The core is gradually warmed up by gravitational contraction, accretion shocks and, eventually, nuclear fusion in the protostar. Volatile species such as CO, CH_4 and N_2 now evaporate from the grains (van Dishoeck et al. 1993, Aikawa et al. 2001, Jørgensen et al. 2002, 2004, 2005, Lee et al. 2004) and this also affects the gas-phase abundances of other species (Chapter 3). The warm-up to 20–40 K further drives a rich grain-surface chemistry (Garrod & Herbst 2006, Garrod et al. 2008, Öberg et al. 2009a; see also the review by Herbst & van Dishoeck 2009). The remaining ice molecules may not be volatile enough at these temperatures to evaporate, but they are mobile enough to diffuse more rapidly across the surface and react with each other. This leads to the formation of so-called first-generation complex organic molecules like HCOOH and $HCOOCH_3$ at point 1 in Fig. 1.2.

As shown by Benson & Myers (1989) and Goodman et al. (1993), cloud cores rotate at a rate of 10^{-14}–10^{-13} s^{-1}. Angular momentum must be conserved throughout the collapse and this results in the formation of a disk around the protostar (Cassen & Moosman 1981, Terebey et al. 1984). Another feature that appears at roughly the same time is a bipolar jet, launched along the core's rotation axis from close to the protostar (Shu et al. 1991, Bally et al. 2007). The jets are probably another mechanism to remove excess angular momentum, but their precise origin remains poorly understood (Ray et al. 2007). They carve out a bipolar cavity in the remnant core material, which at this stage is usually called the envelope. Bipolar cavities have been observed for many protostars (Padgett et al. 1999, Arce & Sargent 2006).

The interaction between the envelope and the circumstellar disk is only understood in the most general terms: material falls in from large radii, hits the disk at some point, and is absorbed by it. It is still an open question whether the accretion from the envelope occurs predominantly onto the inner parts or the outer parts of the disk. The two-dimensional

---

[4] The canonical mass ratio of 0.01 is actually the mass ratio between the dust and the hydrogen gas. The mass ratio between the dust and the total gas is 0.007 (Zhukovska et al. 2008).
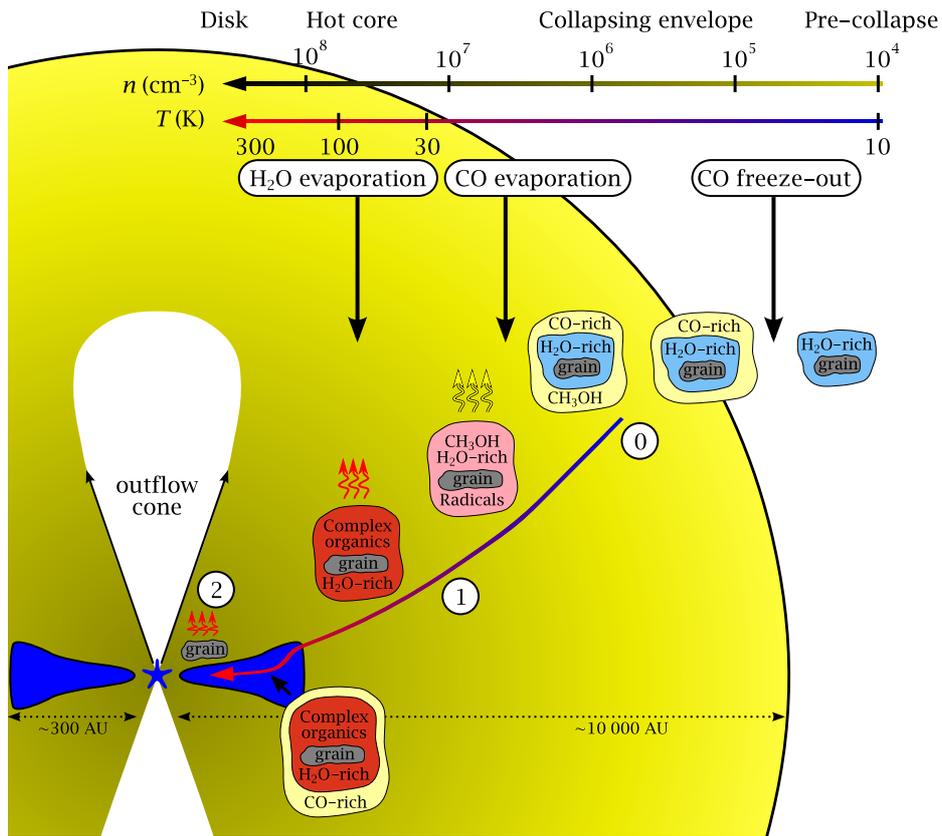
Figure 1.2 – Schematic representation of low-mass star formation and some of the chemistry involved, as reviewed by Herbst & van Dishoeck (2009). CO freezes out before the onset of collapse and is partially hydrogenated to CH_3OH (point 0). As the core warms up during the collapse, CO and other volatiles evaporate and first-generation complex organic molecules are formed on the grains (point 1). Conservation of angular momentum results in the formation of a circumstellar disk, where the temperature may become low enough for CO to freeze out again. In the hot inner region of the core and the disk, the entire ice mantle evaporates and high-temperature reactions in the gas phase lead to a second generation of complex organics (point 2).

(2D) axisymmetric hydrodynamical simulations of Brinch et al. (2008a,b) suggest the latter. As the disk gets thicker (i.e., more vertically extended), material from the envelope would have to flow across the surface of the disk in order to accrete onto the inner part. Brinch et al. showed that this does not typically happen. Instead, most material hits the disk near its outer edge. We also see a lot of envelope material hitting the outer parts of the disk in our semi-analytical collapse model, but there is still a fair amount (up to 50%) that makes its way to the inner parts of the disk and accretes there (Fig. 1.3; see also Fig.
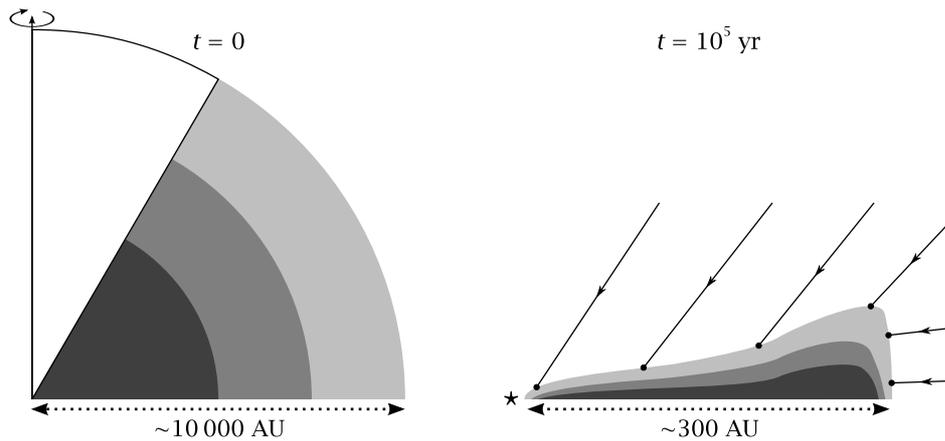
Figure 1.3 – Cartoon view of the layered accretion in one quadrant of our collapse model, based on Fig. 2.7 from Chapter 2. The outer parts of the original cloud core (left) end up as the surface layers of the circumstellar disk (right). The white part of the core is roughly the part that disappears into the outflow. The arrows illustrate the flow of material onto the disk.

4.2 in Chapter 4). Both the hydrodynamical simulations of Brinch et al. and our semi-analytical model result in layered accretion: the inner parts of the original cloud core end up near the midplane of the disk, and the outer parts of the core end up near the surface of the disk (Fig. 1.3; see Chapter 2 for details). Whether this is indeed what happens in reality remains to be confirmed by observations and 3D models.

Depending on initial conditions like the mass of the core and its rotation rate, the disk formed around the protostar can grow as large as 1000 AU (Andrews & Williams 2007b). Its density is several orders of magnitude higher than that of the core – in the inner parts, 10^{12} cm^{-3} is not unusual. Because of the wide range of physical conditions present throughout the disk, there are several distinct chemical regimes (Fig. 1.4). The midplane is shielded from direct irradiation, so the temperature may drop to 10 K or less. The volatile species that evaporated during the initial stages of the collapse now freeze out again onto the cold dust (see also Fig. 1.2, between points 1 and 2). Closer to the surface of the disk, the physical conditions are very different: the density is only 10^6 cm^{-3} or less, the temperature easily exceeds 100 K, and there is a strong UV field from the protostar. Ices cannot survive in such an environment and the first-generation complex organics formed at earlier times are liberated into the gas phase (point 2 in Fig. 1.2). There they can participate in a hot-core chemistry to form a second generation of complex organics (Herbst & van Dishoeck 2009). The same can happen with infalling material that passes through the hot inner part of the remnant envelope.

The entire collapse phase typically lasts a few 10^5 yr. The envelope gradually dissipates towards the end of that period and we are left with a pre-main sequence star surrounded by a circumstellar disk. Depending on the mass of star, it is known in this stage
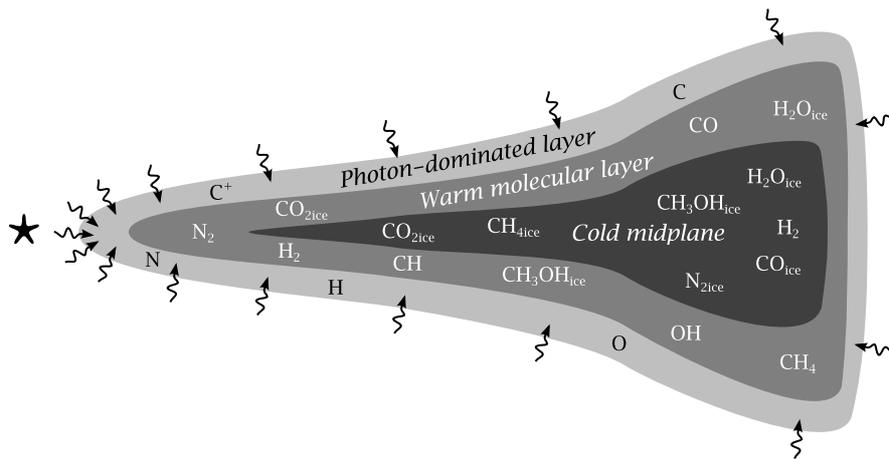
Figure 1.4 – Schematic representation of the three chemical regimes in a circumstellar disk: the photon-dominated layer (irradiated by the protostar and the interstellar UV field), the warm molecular layer, and the cold midplane. Typical species for each regime are indicated.

as a T Tauri ($< 2 \, M_\odot$) or Herbig Ae/Be star (2–$8 \, M_\odot$). The gaseous part of the disk disappears over a period of about 10 Myr by photoevaporation and ongoing accretion onto the star (Hollenbach et al. 2000, Haisch et al. 2001). During that time, its chemistry can roughly be divided into the three regimes shown in Fig. 1.4 (Bergin et al. 2007). It is as yet unknown whether the chemical composition of the disk is purely a result of the physical conditions during the T Tauri or Herbig Ae/Be stage, or whether the disk contains some kind of chemical history from the collapse phase. This is one of the key questions addressed in this thesis.

1.3   Planets, comets and meteorites

The evolution of the dust in the disk is governed by two processes: settling towards the midplane and coagulation into larger grains (Weidenschilling 1980, Miyake & Nakagawa 1995, Dullemond & Dominik 2004b, D'Alessio et al. 2006, Dullemond et al. 2007a, Lommen et al. 2007, 2009; see also the reviews by Natta et al. 2007 and Dominik et al. 2007). Together this may eventually lead to the formation of comets and planets. Whether planets are formed in all circumstellar disks is still an open question. It is also not yet clear how exactly planets are formed: two mechanisms have been proposed (core accretion and gravitational instabilities), but neither of them can be ruled out based on current observations (Matsuo et al. 2007, Lissauer & Stevenson 2007, Durisen et al. 2007).

Regardless of the details of how planets are formed, their initial chemical composition is inherited from the disk. This is also true for comets, and it is these objects in
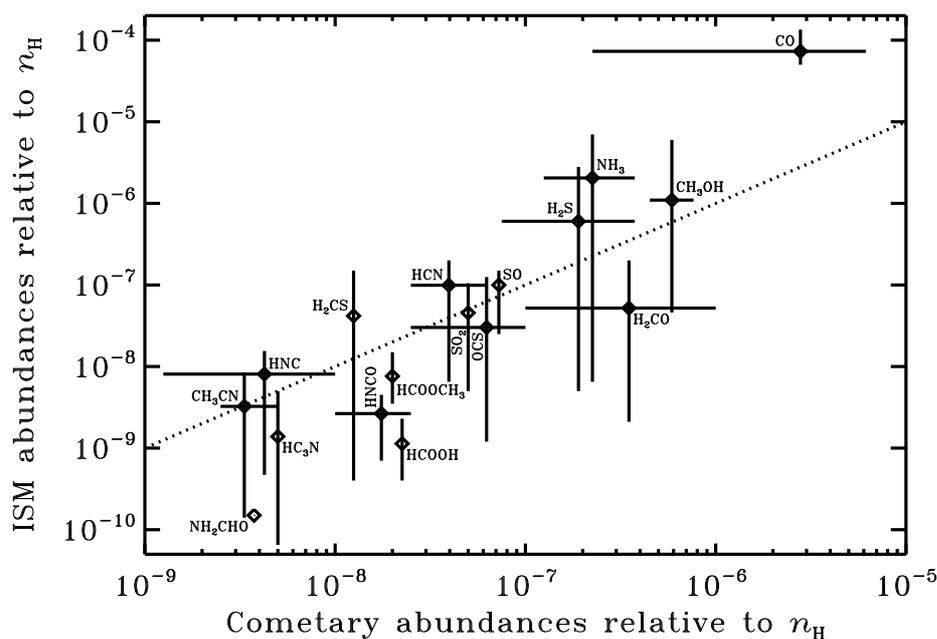
Figure 1.5 – Molecular abundances in comets (Halley, Hale-Bopp, Hyakutake, Lee, C/1999 S4 and Ikeya-Zhang) compared to those in ISM sources (IRAS 16293–2422 (warm inner envelope), L1157, W3(H$_2$O), G34.3+0.15, Orion Hot Core and Orion Compact Ridge) as provided by Bockelée-Morvan et al. (2000, 2004) and Schöier et al. (2002). The error bars indicate the spread between sources; errors from individual measurements are not included. The dashed line represents a one-to-one correspondence between cometary and ISM abundances and is not a fit to the data.

our own solar system that provide the most direct probe of the chemistry of the pre-solar nebula (Bockelée-Morvan et al. 2000). Spectroscopic studies of comet C/1995 O1 (Hale-Bopp) revealed a chemical composition that is remarkably similar to that of interstellar ices, hot cores and bipolar outflows, suggesting that the cometary ices were formed in the ISM and underwent little processing in the solar nebula. However, observations of a dozen other comets show abundance variations of at least an order of magnitude for CO, H$_2$CO, CH$_3$OH, HNC, H$_2$S and S$_2$, as well as smaller variations for other species (Bockelée-Morvan et al. 2004, Kobayashi et al. 2007). In Fig. 1.5, the abundances from the six comets 1P/Halley, Hale-Bopp, C/1996 B2 (Hyakutake), C/1999 H1 (Lee), C/1999 S4 (LINEAR) and 153P/Ikeya-Zhang are compared against those in the embedded proto-star IRAS 16293–2422 (warm inner envelope), the bipolar outflow L1157, and the four hot cores W3(H$_2$O), G34.3+0.15, Orion HC and Orion CR (Bockelée-Morvan et al. 2000, 2004, Schöier et al. 2002). On the one hand, it shows the general correspondence between cometary and ISM abundances. On the other hand, it shows that the abundances can vary

greatly from one comet to the next. These different chemical compositions may be explained by assuming that the comets were formed in different parts of the solar nebula. If that is indeed the case, there must have been some degree of chemical processing between the ISM and the formation of the cometary nuclei. Two-dimensional collapse models such as the one presented in this thesis may help to clarify exactly how chemically pristine the cometary material is and where the mutual differences come from.

Meteorites provide another set of clues about the physical and chemical conditions in the early solar system. For example, Clayton et al. (1973) measured the abundances of the rare oxygen isotopes ^{17}O and ^{18}O in meteorites and found that they could not be explained with normal low-temperature isotope enhancement reactions alone.[5] Recently, this so-called oxygen isotope anomaly has been interpreted as evidence for isotope-selective photoprocesses in the solar nebula – more specifically, for the selective photodissociation of $C^{16}O$, $C^{17}O$ and $C^{18}O$ (Clayton 2002, Lyons & Young 2005, Lee et al. 2008). If true, this would put strong constraints on the ambient UV intensity in the solar neighbourhood around 5 Gyr ago.

1.4 Chemical models

1.4.1 Historical development and reaction types

Chemical models play a pivotal role in interpreting abundances derived from spectroscopic observations. One of the first such models was constructed at Leiden Observatory in 1946 by Kramers & ter Haar and was targeted at CH and CH$^+$, two of the first three molecules detected in the ISM (Sect. 1.1). Other early chemical modelling studies were undertaken by Bates & Spitzer (1951) and Solomon & Klemperer (1972). The latter used a network consisting of 22 monatomic and diatomic species linked by 34 reactions. They obtained good quantitative agreement with the observations of Herbig (1968) of CH and CN along the line of sight towards the star ζ Ophiuchi, but they could not reproduce the abundance of CH$^+$. As observations identified ever more complex species over the years, so chemical networks have expanded. The latest versions of the two most popular networks – UMIST06 and osu_03_2008 – contain about 450 species and 4500 reactions (Woodall et al. 2007, Hersant et al. 2009).[6] However, there are still many scientific questions that can be answered with only a few dozen species and a few hundred reactions (see, for example, Chapters 5 and 6).

The reactions in an astrochemical network can be categorised into several types. Table 1.1 lists the types used in modern networks like UMIST06 and osu_03_2008. The first 14 reaction types belong exclusively to the gas phase; types 15–18 describe gas-grain

---

[5] For a set of isotopologues, the zero-point vibrational energy decreases with increasing mass. Therefore, the abundances of heavy isotopologues like $H_2^{17}O$ and $H_2^{18}O$ are enhanced at low temperature relative to the lighter isotopologue $H_2^{16}O$.

[6] These numbers do not include recent developments like grain-surface chemistry (Hasegawa et al. 1992, Garrod et al. 2008) or hydrocarbon anions (Millar et al. 2007, Walsh et al. 2009), which would make the networks even larger. Adding isotopes like D or ^{13}C would also greatly expand the size of the network.

Table 1.1 – Reaction types in current astrochemical models.[a]

Number	Type[b]	Example
1	*neutral-neutral*	$OH + O \rightarrow O_2 + H$
2	*ion-neutral*	$CH_2^+ + H_2 \rightarrow CH_3^+ + H$
3	*charge exchange*	$CH + C^+ \rightarrow CH^+ + C$
4	mutual neutralisation	$C^+ + H^- \rightarrow C + H$
5	*dissociative recombination*	$CH^+ + e^- \rightarrow C + H$
6	*radiative recombination*	$CH^+ + e^- \rightarrow CH + h\nu$
7	associative detachment	$N + H^- \rightarrow NH + e^-$
8	*radiative association*	$C + H_2 \rightarrow CH_2 + h\nu$
9	*photodissociation*	$CO + h\nu \rightarrow C + O$
10	*photoionisation*	$C + h\nu \rightarrow C^+ + e^-$
11	cosmic-ray dissociation	$H_2 + \zeta \rightarrow H^+ + H^-$
12	*cosmic-ray ionisation*	$H_2 + \zeta \rightarrow H_2^+ + e^-$
13	cosmic-ray–induced photodissociation	$CO + \zeta\text{–}h\nu \rightarrow C + O$
14	cosmic-ray–induced photoionisation	$C + \zeta\text{–}h\nu \rightarrow C^+ + e^-$
15	adsorption (or freeze-out)	$CO \rightarrow CO_{ice}$
16	desorption (or evaporation)	$CO_{ice} \rightarrow CO$
17	grain-surface hydrogenation	$O_{ice} + H \rightarrow OH_{ice}$
18	grain-surface radical-radical	$CHO_{ice} + OH_{ice} \rightarrow HCOOH_{ice}$

[a] Based on Woodall et al. (2007). All species are in the gas phase unless indicated otherwise. The symbols $h\nu$, ζ and $\zeta\text{–}h\nu$ indicate a photon, a cosmic ray and a cosmic-ray–induced photon, respectively.

[b] Reaction types in italics were already included in the model by Solomon & Klemperer (1972).

interactions and grain-surface reactions. It is interesting to note that of the fourteen gas-phase reaction types in Table 1.1, nine were already included by Solomon & Klemperer (1972) in their chemical model. A reaction type of particular importance to this thesis is photodissociation. It is one of the key processes controlling the abundances during the collapse phase in Chapter 3 and it sets a lower limit to the size of circumstellar PAHs in Chapter 6. It plays an even larger role in Chapter 5, which is entirely about the selective photodissociation of CO isotopologues.

Photodissociation can take place in several ways (van Dishoeck 1987, 1988, Kirby & van Dishoeck 1988), two of which are illustrated in Fig. 1.6. For most simple species, the main channel is direct photodissociation. Absorption of a UV or visible photon brings the molecule from the electronic ground state into a repulsive excited state. Spontaneous emission back to the ground state is a slow process, so essentially all absorptions result in photodissociation. The corresponding cross section is a continuous function peaking at the vertical excitation energy. Another possible mechanism is predissociation: the molecule is first excited from the ground state into a bound upper state and then crosses over into a repulsive state. This is the dominant dissociation mechanism for CO and its isotopologues (Chapter 5). The predissociation cross section consists of a series of discrete peaks, corresponding to the vibrational levels of the bound upper state.
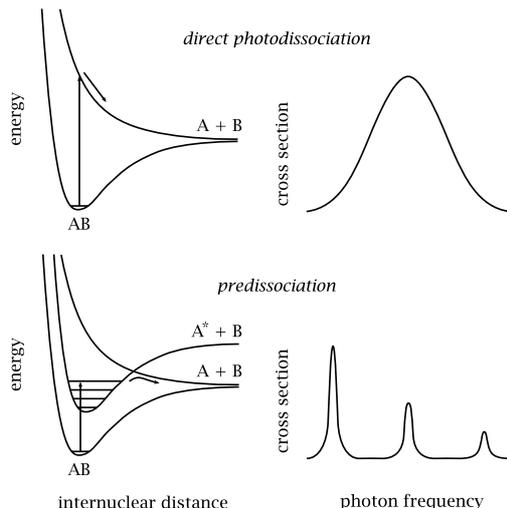
Figure 1.6 – Schematic potential energy curves and cross sections for direct photodissociation (top) and predissociation (bottom) of a diatomic molecule AB, after van Dishoeck (1988).

For molecules with a large number of atoms, such as PAHs (Fig. 1.1), the density of vibrational levels at each electronic state becomes high enough to form a quasi-continuum. When a PAH absorbs a UV or visible photon and is excited to an upper electronic state, it rapidly crosses over into the vibrational quasi-continuum of the electronic ground state (Léger et al. 1988, 1989). From here, it relaxes back to a low vibrational level by radiative decay. As long as the internal energy of the PAH exceeds a certain threshold value, there is the possibility of losing a hydrogen atom or a carbon fragment (Le Page et al. 2001). In the strong radiation fields in the inner parts of the disk and the envelope, the PAH may absorb a second photon before its internal energy falls back below the dissociation threshold. Multi-photon absorptions keep the PAH at high internal energy, thus greatly increasing the effective photodissociation rate (Chapter 6).

1.4.2 Solution methods

Mathematically, a network of chemical reactions results in a system of ordinary differential equations (ODEs). Each species i is formed by a certain number of reactions (say, m_f) and it is destroyed by a certain number of other reactions (say, m_d). Hence, the time derivative of the number density (n_i in cm^{-3}) is

$$\frac{\mathrm{d}n_i}{\mathrm{d}t} = \sum_{j=1}^{m_f} R_{f,j} - \sum_{j=1}^{m_d} R_{d,j}, \qquad (1.1)$$

with $R_{f,j}$ and $R_{d,j}$ the rates (in cm^{-3} s^{-1}) of the individual formation and destruction reactions. If a reaction involves two reactants with number densities n_1 and n_2, its rate is of

the form

$$R = k n_1 n_2 \,. \tag{1.2}$$

This is the case for reaction types 1–8, 17 and 18 from Table 1.1. For types 9–16, where there is only one reactant, the rate is of the form

$$R = k n_1 \,. \tag{1.3}$$

Because of the low densities in most astronomical objects of interest to chemical modellers, reactions with three reactants are very slow and are not included in the standard networks. However, they start to become important in the innermost regions of circumstellar disks.

The variable k in Eqs. (1.2) and (1.3) is the so-called rate coefficient. Rate coefficients are obtained most reliably by measuring the reaction in controlled conditions in a laboratory – ideally at a range of conditions, so that it can be established quantitatively how the coefficient depends for example on temperature. Another good method is to derive the coefficient from quantum chemical state-to-state calculations. However, both methods are time-consuming, so many coefficients in current networks are based on extrapolations or chemical kinetic theories, and some of them are no more than educated guesses.

Given a set of species, reactions and rate coefficients, there are two ways of solving for the abundances: find an equilibrium or follow the evolution of the abundances in time. The two methods are now illustrated with a very simple system consisting of only two species (CO gas and CO ice, with number densities n_{gas} and n_{ice}) linked by two reactions (freeze-out and evaporation, with rates R_{des} and R_{ads}), similar to what is used in Chapter 2. The rate coefficients depend on the temperature T and the gas density n_{H}; we approximate them as

$$k_{\text{ads}} = (1 \times 10^{-18} \text{ cm}^3 \text{ K}^{-1/2} \text{ s}^{-1}) n_{\text{H}} \sqrt{T} \,, \tag{1.4}$$

$$k_{\text{des}} = (1 \times 10^{12} \text{ s}^{-1}) \exp\left(-\frac{855 \text{ K}}{T}\right), \tag{1.5}$$

after Charnley et al. (2001) and Bisschop et al. (2006).

If we are interested in the equilibrium abundances at a given T and n_{H}, we have to solve the equations

$$\begin{cases} \mathrm{d}n_{\text{gas}}/\mathrm{d}t = k_{\text{des}} n_{\text{ice}} - k_{\text{ads}} n_{\text{gas}} = 0 \\ \mathrm{d}n_{\text{ice}}/\mathrm{d}t = k_{\text{ads}} n_{\text{gas}} - k_{\text{des}} n_{\text{ice}} = 0 \end{cases} \tag{1.6}$$

under the condition of conservation of mass. Setting the total CO abundance to 10^{-4} relative to n_{H}, this is simply expressed as

$$n_{\text{gas}} + n_{\text{ice}} = 10^{-4} n_{\text{H}} \,. \tag{1.7}$$

The equilibrium solution then becomes

$$n_{\text{gas}} = \frac{10^{-4} n_{\text{H}} k_{\text{des}}}{k_{\text{ads}} + k_{\text{des}}} \,, \qquad n_{\text{ice}} = 10^{-4} n_{\text{H}} - n_{\text{gas}} \,. \tag{1.8}$$

13

The procedure is essentially the same for a full chemical network: set the time derivatives of all individual abundances to zero and ensure conservation of mass. However, an analytical solution can generally not be derived for a full network. Instead, the problem must be solved with a numerical procedure like the Newton-Raphson routine (Press et al. 1992).

Solving for the equilibrium abundances is usually fine if the physical conditions are constant, although one always has to check that the object of interest is old enough to reach chemical equilibrium. If that is not the case, or if the physical conditions change on timescales shorter than the chemical timescale, one has to solve the abundances time-dependently with an integration package like VODE (Brown et al. 1989). Starting from some initial values, the abundances are evolved in small time steps Δt up to a pre-determined final time. Turning back to our CO system, we could for example begin with all CO as ice and ask how long it takes to evaporate at $n_\mathrm{H} = 10^4$ cm^{-3} and $T = 18$ K. We could also simulate the warm-up phase during the collapse of a cloud core by starting at 10 K and increasing the temperature at a typical rate of 0.01 K yr^{-1}. If we couple this to a physical model of the collapse to get a relationship between the temperature and the distance from the protostar, we could then say *where* CO evaporates. Finally, we could add other molecules to the mix and expand the simple freeze-out/evaporation scheme to a full chemical network. In essence, this is what we do in Chapters 2 and 3.

1.5   This thesis

The central theme of this thesis is the chemical evolution during the formation of low-mass stars and their surrounding disks. Although the initial stages of the collapsing cloud core are well described by spherically symmetric models, this is no longer possible once the disk is formed. So far, the chemistry during the collapse phase has only been studied up to the point that the disk is formed or on large scales where spherical symmetry can still be safely assumed (> 1000 AU). In this thesis we present the first physical-chemical model that follows the entire core collapse and disk formation process in two dimensions.

In the preceding sections we introduced several open questions related to low-mass star formation and the chemical evolution of the material involved. The most important ones addressed in this thesis are:

- Does material from the envelope accrete predominantly on the inner or on the outer parts of the disk?
- How does the chemical composition of the gas and dust change from the envelope to the disk?
- Is the chemical composition of a T Tauri or Herbig Ae/Be disk purely a result of in situ processes or does it retain some signature of the collapse phase?
- What fraction of the cometary ices is truly pristine?
- What is the origin of the chemical diversity of comets?

The first three chapters of this thesis deal with our 2D collapse model. To begin with, Chapter 2 contains a full description of the model. We couple the analytical collapse solu-

tions of Shu (1977), Cassen & Moosman (1981) and Terebey et al. (1984) to the model of Lynden-Bell & Pringle (1974) for a viscously evolving circumstellar disk. The size and luminosity of the central sources evolve according to Adams & Shu (1986) and Young & Evans (2005). We define a standard set of initial conditions (core mass, sound speed and rotation rate) and find that the resulting density and velocity profiles show good agreement with those from more detailed hydrodynamical simulations (Yorke & Bodenheimer 1999, Brinch et al. 2008a,b). The temperature is a very important input parameter for the chemistry, so we compute it with a full radiative transfer method (Dullemond & Dominik 2004a) at a series of time intervals. The semi-analytical nature of our model allows us to easily change the initial conditions and we obtain density, velocity and temperature profiles for a small grid of parameters.

As a first illustration of the full chemistry, we look at the freeze-out and evaporation of CO and H_2O. We calculate infall trajectories originating from several thousand points in the cloud core to see how material flows towards the star and the disk. The density and temperature along each trajectory provide the input for evolving the gas and ice abundances of CO and H_2O, resulting in 2D profiles of the gas-to-ice ratios in the disk and remnant envelope.

In Chapter 4, we revisit one particular physical aspect of our collapse model: the sub-Keplerian velocity at which material accretes onto the disk. This problem was studied previously by Cassen & Moosman (1981) and Hueso & Guillot (2005), but not in the context of a 2D model. We derive a new solution for the radial velocities inside the disk and show that it does not strongly affect the results from the preceding chapter. However, it does offer new insights into the related question of why the dust in circumstellar disks is more crystalline than in the ISM. We rerun the models of Dullemond et al. (2006a) and obtain a better match with observed crystalline abundances in disks.

We couple our 2D collapse model – including the new correction for sub-Keplerian accretion – to a full gas-phase chemical network in Chapter 3 to analyse the abundances of several major oxygen-, carbon- and nitrogen-bearing species. We describe the evolution of the abundances along one specific infall trajectory and show that most changes can be traced back to key chemical processes like the evaporation of CO or the photodissociation of H_2O. In turn, these key processes relate back to physical events like the increase in temperature or UV flux at some point along the trajectory. Material ending up in other parts of the disk encounters different physical conditions and we show how that affects the abundances of certain species. Finally, we seek to answer whether the disks around T Tauri and Herbig Ae/Be stars retain some signature of the collapse-phase chemistry, or if their chemical composition is fully determined by in situ processing. To that end, we evolve the abundances obtained at the end of the collapse for another 1 Myr in a static disk model to see how much they still change.

Having discussed the gas-phase chemistry and the dust mineralogy, we turn to the question of isotopes in Chapter 5. We derive an extensive update to the CO photodissociation model of van Dishoeck & Black (1988) using new laboratory data. The model includes not only the regular isotopes ^{12}C and ^{16}O, but also the less abundant ^{13}C, ^{17}O and ^{18}O. We discuss the effect of the temperature on the isotope-selective photodissociation rates and we couple the photodissociation model to a small chemical network to

15

analyse the abundance of CO and its isotopologues as a function of depth into diffuse clouds, photon-dominated regions and circumstellar disks. A long-standing puzzle in our own solar system is the anomalous oxygen isotope ratio found in meteorites. Our results support the recent hypothesis by Lyons & Young (2005) that the anomalous ratio is due to CO photodissociation in the solar nebula.

The final chapter of this thesis targets the chemistry of yet another class of compounds: polycyclic aromatic hydrocarbons or PAHs. We adapt the chemistry models of Le Page et al. (2001) and Weingartner & Draine (2001) and the excitation model of Draine & Li (2007) to find the dominant charge and hydrogenation states of PAHs in disks around T Tauri and Herbig Ae/Be stars. We explicitly calculate where in the disk PAHs are photodissociated, taking into account the possibility of multi-photon absorption events. The 2D abundance profiles thus obtained are coupled to a radiative transfer package (Dullemond & Dominik 2004a) to simulate spatially resolved spectra. Finally, we compare the predicted spatial extent of the PAH features to observations by van Boekel et al. (2004), Habart et al. (2006) and Geers et al. (2007) to determine the size of the PAHs responsible for the observed emission.

Each of the Chapters 2–6 closes with a summary of the conclusions that we draw from our model results and the comparison with observations and other models. We present here the main conclusions from this thesis.

- Our two-dimensional semi-analytical collapse model produces realistic density and velocity profiles, allowing us to track the chemistry all the way from pre-stellar cores to circumstellar disks. Combined with full radiative transfer to get temperatures and UV fluxes, this makes it an excellent tool to study the chemical evolution during low-mass star formation (Chapters 2 and 3).

- Both CO and H_2O freeze out before the onset of collapse. H_2O remains frozen throughout the collapse phase, except when it gets into the inner 5–10 AU of a disk. From there, it may move outwards again to colder regions as the disk expands to conserve angular momentum. CO rapidly evaporates once the collapse starts, although some of it is likely to be trapped in the H_2O ice. In the coldest parts of a disk (< 18 K), all CO freezes out again (Chapters 2 and 3).

- The chemistry during the collapse of a cloud core and the formation of a disk is dominated by a small number of key chemical processes that are activated by changes in the physical conditions. Examples of these key processes are the evaporation of CO, CH_4 and H_2O at approximately 18, 22 and 100 K, and the photodissociation of CH_4 and H_2O in the vicinity of the outflow wall. The photodissociation of CO requires a stellar temperature of at least 7000 K or a colder star with excess UV emission (Chapter 3).

- Because of the short dynamical timescales, the chemistry does not reach equilibrium at any time during the collapse. The chemical composition of the disk at the end of the collapse phase is therefore primarily a product of the physical conditions at earlier times. Additional work is required to determine if any chemical signatures from the collapse phase survive into the T Tauri or Herbig Ae/Be stages (Chapter 3).

16

- The material from which solar-system comets are formed must be of mixed origins. Our collapse model predicts a large degree of chemical processing towards the comet-forming zone in the disk. The observed fractions of crystalline silicates in comets are also indicative of strong processing. However, strong processing cannot explain why the chemical composition of cometary ices so closely resembles that of interstellar ices. The detections of amorphous silicates in comets also point at the presence of unprocessed material. Hence, it would seem that comets were formed partially from processed material and partially from pristine material (Chapters 3 and 4).

- The chemical diversity between individual comets is likely a result of them having formed at different locations in the solar nebula. The physical conditions in a disk change in time, so if two comets were formed several 10^4 or 10^5 yr apart, their chemical compositions would also be different (Chapter 3).

- It is important to take the vertical structure of a disk into account when computing the infall trajectories. The outer parts of a disk can intercept material and keep it from accreting onto the disk at much smaller radii, as it would if the disk is treated as completely flat (Chapters 2–4).

- Thermal annealing followed by outward radial mixing is responsible for at least part of the crystalline silicates observed in circumstellar disks (Chapter 4).

- The CO photodissociation rate obtained with our new model is 30% higher than the old value. The dissociation of $C^{17}O$ and $^{13}C^{17}O$ shows almost exactly the same depth dependence as that of $C^{18}O$ and $^{13}C^{18}O$, respectively, so ^{17}O and ^{18}O are equally fractionated with respect to ^{16}O. The level of fractionation is higher for cold gas than it is for warm gas (Chapter 5).

- Isotope fractionation in circumstellar disks through the photodissociation of CO in the surface layers requires a far-UV component in the irradiating spectrum. The interstellar radiation field is sufficient for this purpose. Our model supports the hypothesis that the photodissociation of CO is responsible for the anomalous ^{17}O and ^{18}O abundances in meteorites (Chapter 5).

- PAH emission from circumstellar disks is extended on a scale similar to the size of the disks. Neutral and positively ionised PAHs contribute to the emission in roughly equal amounts. Based on the spatial extent, the observed emission originates mostly from PAHs with a size of at least 100 carbon atoms. Smaller PAHs are efficiently destroyed by the stellar UV field in the inner ~30 AU of a disk (Chapter 6).

Although our two-dimensional semi-analytical collapse model is an important step forwards in the study of the chemical evolution during low-mass star formation, many questions still remain unanswered. With regards to the model itself, we have only undertaken some basic tests against observations. One of the first challenges now is to couple the model to a radiative transfer package to predict spectral lines and compare them to observational data. The start of science operations with the Herschel Space Observatory later this year and with the Atacama Large Millimeter/submillimeter Array (ALMA) in

2011 offers both exciting possibilities and additional challenges. For example, the unprecedented spatial resolution of ALMA may well require a revision of the physics in the inner parts of the disk and envelope.

Given the semi-analytical nature of our model, some physical aspects had to be simplified. The bipolar outflow is only included in an ad-hoc fashion and we may be underestimating how much material it sweeps up and out of the system. Another simplification involves the amount of core material that becomes involved in the collapse. We currently let the entire core accrete onto the star and disk, but recent interferometric observations call this into question (Jørgensen et al. 2007). In both cases, the final disk mass and temperature would be different, and some of the chemistry would change as well.

On the chemical side, the treatment of photoprocesses currently involves several approximations in the way the shape of the irradiating spectrum is taken into account. Also, grain-surface processes are still largely unexplored. They have to be added to our network if we want to reproduce the observed abundances of methanol and more complex organic molecules. If amino acids and other biologically important species are formed in circumstellar disks, it is likely that this happens on grain surfaces, or that this at least requires precursor molecules formed on grains. In either case, grain-surface chemistry promises to be important as astronomers worldwide continue to unravel the history of our solar system in general and the origins of life on Earth in particular.